Journal of Thermal Engineering, Vol. 6, No. 4, pp. 619-632, July, 2020
Yildiz Technical University Press, Istanbul, Turkey

FEASIBILITY OF GLYCERIN/Al_2O_3 NANOFLUID FOR AUTOMOTIVE COOLING APPLICATIONS

Kondru Gnana Sundari[1], Lazarus Godson Asirvatham[1,*], Joseph John Marshal S[1], Emerald Ninolin[1], Surekha B[2]

ABSTRACT

In this paper, the feasibility of glycerin/Al_2O_3 nanofluid for automotive cooling applications is experimentally studied. The test setup includes an engine model and a car radiator and the heat transfer characteristics at required operating conditions are analyzed under laminar flow conditions. Three different concentrations of nanofluids such as 0.05, 0.1 and 0.15 vol. % are used and the enhancement in the heat transfer coefficient is 62% when 0.15% volume concentration of nanoparticles are added to the base fluid (glycerin) at a constant heat flux of 6919 W/m^2. The effectiveness of the radiator cooling system increases along with negligible increase in pumping power with increase of volume concentration. The addition of nanoparticles in the base fluid enhances the absorption capacity of the radiator coolant leading to the increase in the effectiveness. Results have also indicated that the nanofluids are mainly dependent on particle concentration, flow rates, and temperature. Hence, it is suggested that nanoparticle suspended coolants are promising and efficient for automotive cooling applications.

Keywords: *Nanofluid, Glycerin, Radiator, Convective Heat Transfer Coefficient, Automotive Cooling*

INTRODUCTION

Heat transfer applications play a very vital role in the aspect of energy crisis and energy consumption. Heat transfer enhancement is a major concern in the field of Automobile Industry. Due to the increasing petroleum costs, researchers are motivated to apply energy saving methods. It is mentioned that car radiators are essential accessories for automobiles, so higher heat transfer performance of radiators ensures a high efficiency engine, which leads to smaller engine size, better fuel economy and less emission of gases [1] . For many years water, ethylene glycol and glycerol have been used as conventional coolants in automobile radiator [2,3]. The ASTM Engine Coolant Grade has approved glycerin (D7640, D7714, and D7715 specifications) for light and heavy-duty vehicles as a coolant in April 2011. The glycerin-based coolants are better for the environment as they are close to neutral on a corrosive scale, less corrosive to engine parts and more cost-effective than Ethylene Glycol (commonly used conventional coolant) and supportive of the renewable fuel industry. Glycerin is considered as a Greener Alternative to Ethylene Glycol as Antifreeze (Mark Bateman, Benchmark Energy, 2014). The commercial coolants available in the market are limited by their heat transfer characteristics (low thermal conductivity). This prompted researchers to find fluids that offer higher thermal conductivity compared to that of conventional coolants. For the first time a colloidal mixture of nanoparticles (1-100nm) in a base liquid is prepared by calling it as nanoparticle fluid suspensions [4]. The presence of nanoparticles in the base fluid contributes better flow of mixing and higher thermal conductivity compared to that of a base fluid. When nanoparticles dispersed uniformly and suspended stably in a base fluid can provide impressive improvements in the thermal properties of the base fluid [5] . The purpose of dispersing nanoparticles into conventional coolants (water, ethylene glycol, and glycerol) to increase the efficiency of the engine and their performance has been acknowledged [6]. This resulted in an innovative idea to use nanoparticles in the conventional engine coolants. The thermal fluid by suspending nano size particles in the conventional fluids is a redesigned model for upcoming coolants [7]. Addition of solid nanoparticles into the heat transfer media has been an unique technique for enhancing the heat transfer rate and performance of engines. Many kinds of metallic nanoparticles, such as Al_2O_3, CuO, Fe_2O_3, SiO_2 and TiO_2 were used as additives of base fluids [8–14] Among these metallic nanoparticles Al_2O_3 is

This paper was recommended for publication in revised form by Regional Editor Balaram Kundu
[1] Department of Mechanical Engineering, Karunya Institute of Technology and Sciences, Coimbatore, Tamil Nadu, India
[2] Department of Mechanical Engineering, Kalinga Institute of Industrial Technology, Bhubaneswar, Odisha, India
**E-mail address: godson@karunya.edu*
Orcid id: 0000-0001-6323-8479
Manuscript Received 05 April 2018, Accepted 27 May 2018

one of the most commonly studied nanoparticles in commercial coolants. Numerous studies were reported in the literature with Al_2O_3/water nanofluid in a vehicle cooling system. An enhancement of 14.79%, 14.72%, and 9.51% respectively is observed in heat transfer rate, heat transfer coefficient and Nusselt number for 1 vol. % of nanoparticle concentration [15]. It is mentioned the maximum enhancement of heat transfer for 1 vol. % is found 52.03% higher when compared with water [16]. The enhancement observed is 3% and 40-45 % maximum enhancement in thermal conductivity and heat transfer respectively for 1 vol. % [17]. When 2 vol. % was considered it is reported heat transfer coefficient enhancement is up to 25% [18]. It is experimentally proved that the maximum heat transfer coefficient increased 41% in the entry length by dispersing nano particles [19]. An experimental study of Al_2O_3/EG nanofluids in vehicle cooling system is performed and reported thermal conductivity enhancement of 11.25%, when 3.5% and 4.5 % enhancement with 1.5 vol. % of nanoparticles addition [20]. The maximum increase in the thermal conductivity was 8.3%, when 1 vol. % of Al_2O_3 nanoparticles are added to EG at 50°C [21]. An increase in thermal efficiency by 14.4% when 2 vol. % of Al_2O_3 nanoparticles were added in EG/Water coolant. Some experimental results demonstrated that the heat transfer behaviors were highly dependent on the particle concentration and the flow conditions and weakly dependent on the temperature [22]. He observed heat transfer enhancement of 40% in a range of 0.1-1 vol. % of gamma-alumina nanoparticles added to different base fluids (5, 10, 20 vol. % of EG). Yu et al. [23] focused his study on Al_2O_3 nanofluid (45% ethylene glycol and 55% water mixture as base fluid) and found the values of heat transfer coefficient of nanofluids enhanced up to 57% and 106% for 1.0 vol. % and 2.0 vol.%, when the Reynolds number is 2000 [24].The nanofluids with Al_2O_3 has an notable enhancement of thermal conductivity in the range of 2-36% [25].

It is observed that so far in the literature works have not been reported with Al_2O_3 nanoparticles suspended in glycerin-based coolant. Therefore, an experimental study is carried out to estimate heat transfer coefficient and friction factor at three different volume concentrations of glycerin/Al_2O_3 nanofluids under laminar flow conditions using a compact engine model and an air-cooled radiator.

EXPERIMENTATION

Preparation and Characterization of Nanofluid

The Al_2O_3 nanoparticles with diameters <50nm purchased from Alfa Aesar, UK (ASP Powder, LOT-E26XO39) is used for experimental work. The volumetric concentrations varied from 0.05%, 0.1% to 0.15% throughout the experimental process. All the properties are recorded without using the surfactant in the nanofluid. Hielscher UP400S AT 70 Hz is used for ultra-sonication for 30, 60,120 minutes and best results are noted for 120 minutes. The stability of the nanofluid is checked by keeping the prepared nanofluid idle for one week and physically observed for any settlement of nanoparticles at the bottom of the container. It is observed that the nanoparticles are stably suspended in the base fluid even after one week. The average crystallite size of the sample is calculated by measuring the broadening of the X-ray diffraction peaks and applying the Debye-Scherrer's formula and given in Equation 1. The crystalline size of the sample is calculated as 12.824 nm as shown in Figure 1.

Measurement of thermophysical properties of nanofluid

The thermo-physical properties like thermal conductivity, viscosity, pH, Surface Tension of the nanofluids were experimentally studied. The thermal conductivity is measured by using KD2- Pro thermal properties analyzer (made by Decagon, USA). It ensured that the accuracy of the analyzer is ±0.1. The viscosity of the nanofluids was measured by using Brookfield DV-III ultra-programmable Rheometer. The Surface tension of the nanoparticles was measured by using bubble pressure tensiometer, where the force measurement is done between the probe and the interface of the fluid. The instrument used to calibrate the pH of the nanofluid is Elico LI 120, range 0-14, repeatability 0.01, accuracy ±0.0001 and maintains the stability of ±0.005 in 5 hours. The results are presented elsewhere by the same author [27].

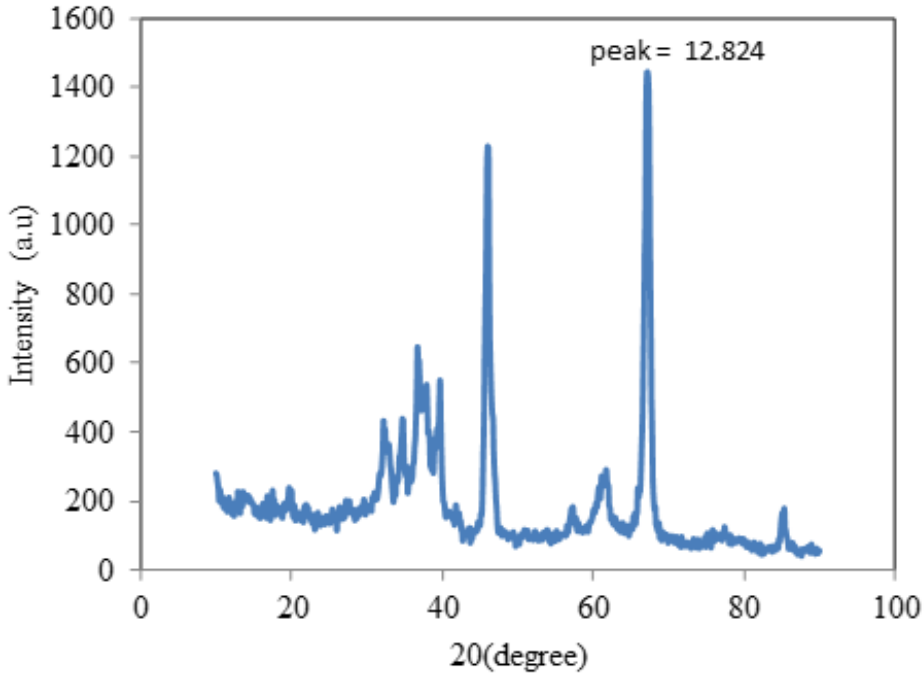

Figure 1. X-Ray Diffactrogram of alümina nanoparticles

Experimental Setup

The schematic diagram of the experimental setup as shown in Figure 2 is fabricated to measure the heat transfer coefficient and pressure drop (Δp) of the nanofluid. The setup has a steel reservoir tank of 3 liters capacity of 22cm width and 22cm in height for the nanofluid and a centrifugal pump to pump the nanofluid throughout the experimental setup. For measurement of temperature sixteen thermocouples are fixed on the test section of the heater and the radiator.

The thermocouples (T type) are fixed at the inlet and the outlet of the heater test section and four thermocouples are fixed on the wall at 0.07m,0.19m,0.31m, and 0.43m distance of the 0.5m long test section. Two thermocouples are placed at the inlet and outlet of the radiator and eight thermocouples are placed on the wall of the radiator. A tube of 2.54cm diameter and 50 cm in length is considered as an engine model on which a circumferential heater is provided with a constant heat flux to heat the liquid in the tube. The power of the heater can be adjusted by a Variac (0-270V) in which the voltage can be adjusted to supply the required power to the heater. The test section is completely insulated on both sides with ceramic wool. A flow meter (10-500 LPH) is used and two needle valves are used to regulate the flow rate of the test fluid. The working fluid is initially poured into the reservoir tank and 1.5 liters of fluid is kept constantly circulating in the entire test setup. The car radiator has a fan (1500rpm) attached to the airside and provided with a DC supply to turn on the fan. To measure the pressure at the inlet and outlet of the heater test section two micro-preamp (EN837-1) pressure gauges are fixed. A drain valve is fixed under the reservoir tank for cleaning and changing the nanofluid.

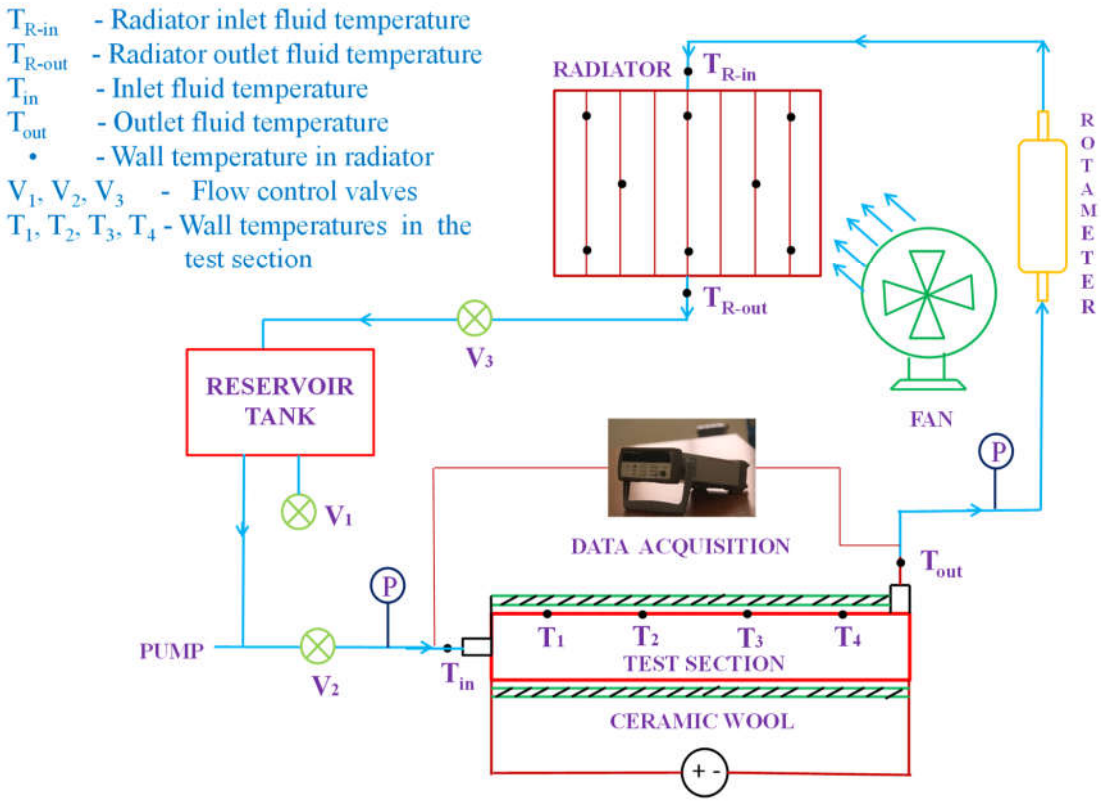

Figure 2. Schematic diagram of the experimental setup

Experimental Procedure

The working fluid is taken as G13 (G O13 A8J M1) which is an engine-based coolant and is used as a base fluid in the entire experimental setup. The engine coolant is mixed with water at 50:50 ratio. The Al_2O_3 nanoparticles at 0.05%, 0.1% and 0.15% volume concentrations are dispersed in the engine coolant. The thermocouples are connected to the data logger (YOKOGAWA – N 200, Model – DA 100-13-1F) for the measurement of temperature. The leak test is done prior the experiment by pumping water through the entire test setup and no leakage is found. The heating input of 6919 W/m^2 is given as a constant heat flux throughout the experimental conditions. The readings are taken at ambient temperature to check the thermocouples reading in the sixteen thermocouples. By increasing the mass flow rate at a constant heat flux of 6919 W/m^2, the readings are noted for different volume concentrations. The steady state readings are taken at the end of every flow rate.

Data Reduction

The average crystalline size of the sample is calculated by measuring the X- Ray diffraction peaks of the nanoparticles by applying the Debye- Scherrer's formula which is given in Equation 1.

$$D_{vol} = \frac{k\lambda}{\beta \cos\theta} \tag{1}$$

In which the $D_{vol.}$is the volume weighed crystallized diameter of the equivalent spherical particles and the Scherrer constant, *k* (value ranging from 0.892-1.4, for Al_2O_3, k value is1.2), λ is the wavelength of the x-ray source (0.15406 run). β Value is the full width at half maximum (radian) and θ is the half of the diffraction angle.
The heat transfer coefficient of the nanofluids was calculated using the following convective heat transfer coefficient (h_i) as in Equation 2.

$$h_i = \frac{q}{\left(T_{W(i)} - T_{f(i)}\right)} \tag{2}$$

Where q is the heat flux and $T_{w(i)}$ and $T_{f(i)}$ are the respective wall and fluid temperatures at that local point in the pipe. The axial profile of a local heat transfer coefficient of the glycerin Al_2O_3 nanofluid with varying volumetric concentrations is obtained by the energy balance Equation 3.

$$T_{f(i)} = T_{in} + \frac{qS_x}{(\rho C_p v A)} \tag{3}$$

Where T_{in} is the inlet fluid temperature, ρ is the fluid density, A is cross-sectional area of the tube, S_x is the perimeter of the test section, C_p is the specific heat capacity of the fluid and v is the fluid velocity.
The effect of wall and bulk temperature (T_{bulk}) on the axial length with varying volumetric concentrations is obtained from the Equations 4 and 5.

$$T_{bulk} = \left(\frac{T_{f(i)} + T_{in}}{2}\right) \tag{4}$$

$$T_w = \frac{T_1 + T_2 + T_3 + T_4}{4} \tag{5}$$

Where T_W is average wall temperature and T_1, T_2, T_3, T_4 are the respective wall temperatures on the test sections.

The variation of average heat transfer coefficient (h_{avg}) as a function of Reynolds number is calculated by the Equation 6.

$$h_{avg} = \frac{(h_i)_1 + (h_i)_2 + (h_i)_3 + (h_i)_4}{4} \tag{6}$$

Where $(h_i)_1$, $(h_i)_2$, $(h_i)_3$, $(h_i)_4$ are the local heat transfer coefficient of the test sections.
The effect of effectiveness with respective to the Reynolds number is calculated by Equation 7.

$$\varepsilon = \frac{m_h c_h}{C_{min}} \left[\frac{T_1 - T_2}{T_1 - t_1}\right] \tag{7}$$

The influence of the radiator outlet temperature with respective to the Reynolds number is calculated from the Equation 8.

$$(mC_p \Delta T)_W = (mC_p \Delta T)_{Air} \tag{8}$$

Uncertainty Analysis

The propagation analysis provides an easy way to calculate the uncertainty in the analyzed results of Ahammed et al.[28] from Equations 9 to 12. The uncertainty values of the experimentally measured properties are taken into consideration. The sources of measurement errors are analyzed and the values of uncertainty of the measured quantities of flow rate are ±3.5%, Reynolds number ±2.01%, heat flux ±1.34% and heat transfer coefficient ± 1.81%.

$$\frac{\delta Q_c}{Q_c}=\left[\left(\frac{\delta m}{m}\right)^2+\left(\frac{\delta C_p}{C_p}\right)^2+\left(\frac{\delta\left(T_\infty-T_c\right)}{\left(T_\infty-T_c\right)}\right)^2\right]^{1/2} \tag{9}$$

$$\frac{\delta Q_{in}}{Q_{in}}=\left[\left(\frac{\delta V}{V}\right)^2+\left(\frac{\delta I}{I}\right)^2\right]^{1/2} \tag{10}$$

$$\frac{\delta Q_h}{Q_h}=\left[\left(\frac{\delta Q_c}{Q_c}\right)^2+\left(\frac{\delta Q_{in}}{Q_{in}}\right)^2\right]^{1/2} \tag{11}$$

$$\frac{\delta h}{h}=\left[\left(\frac{\delta Q_h}{Q_h}\right)^2+\left(\frac{\delta D_h}{D_h}\right)^2+\left(\frac{\delta L}{L}\right)^2+\left(\frac{\delta\left(T_w-\frac{T_w+T_{in}}{2}\right)}{\left(T_w-\frac{T_w+T_{in}}{2}\right)}\right)^2\right]^{1/2} \tag{12}$$

Where V and I are voltage and current, L and D are respective length and diameter of the test section.

RESULTS AND DISCUSSION

Influence of Thermal Conductivity and Viscosity

Figure 3 shows the variation in thermal conductivity and viscosity with temperature. It is observed that the thermal conductivity increases with increase in temperature of Al_2O_3 nanoparticles. The enhancement in thermal conductivity of the nanofluid for a volume concentration of 0.1% is found to be 19.52% and 46.15% as the temperature increases from 30ºC to 50ºC. Similarly, the enhancement in thermal conductivity for a volume concentration of 0.15% is observed to be 38.57% and 52.50%. Therefore, the thermal conductivity increases as the concentration of nanoparticles increases from 0.1% to 0.15%. An enhancement in thermal conductivity of 52.50% has been observed for 0.15% volume concentration of glycerin/Al_2O_3 nanofluid when compared to the base fluid at 50ºC. The enhancement in thermal conductivity of nanofluid is because of the vigorous particle movement during the rise of temperature. As the temperature increases from 30ºC to 50ºC, the viscosity of the glycerin/Al_2O_3 nanofluid decreases. The graph shows a variable decrease of viscosity as the temperature increases. For example, with a concentration of 0.05% the viscosity value decreases from 0.904mPa s to 0.616mPa s as the temperature increases from 30ºC to 50ºC. For 0.05%, 0.1% & 0.15% of volume concentrations of nanofluid, the average reduction is about 31%, 30% & 29% respectively as the temperature increases from 30ºC to 50ºC. The reason for the decrease in viscosity of the nanofluid is due to the increase in temperature. The shear force between the layers decreases, which results in the reduction of viscosity.

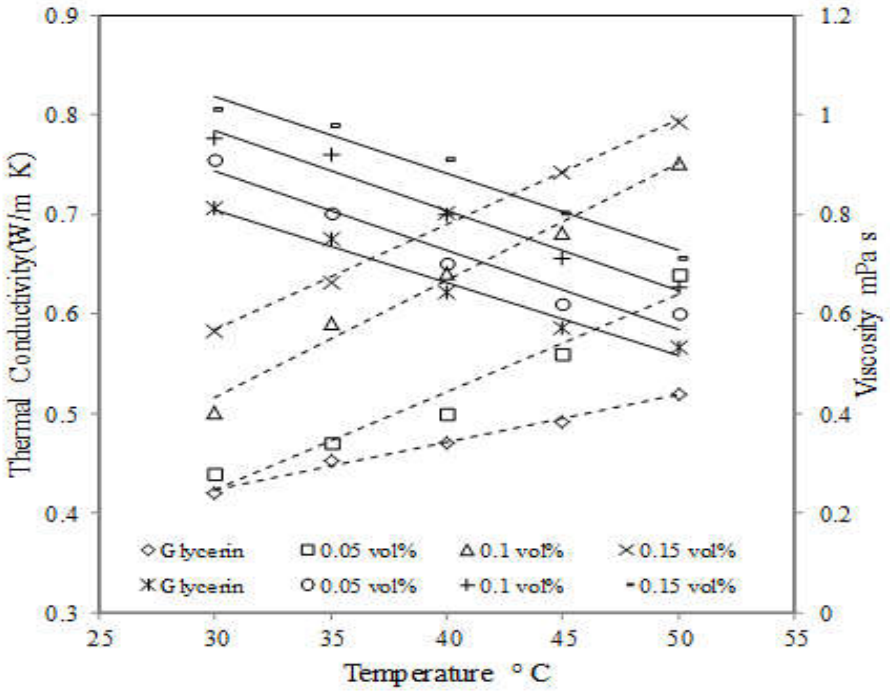

Figure 3. Thermal conductivity and viscosity of glycerin/Al_2O_3 nanofluid as a function of temperature

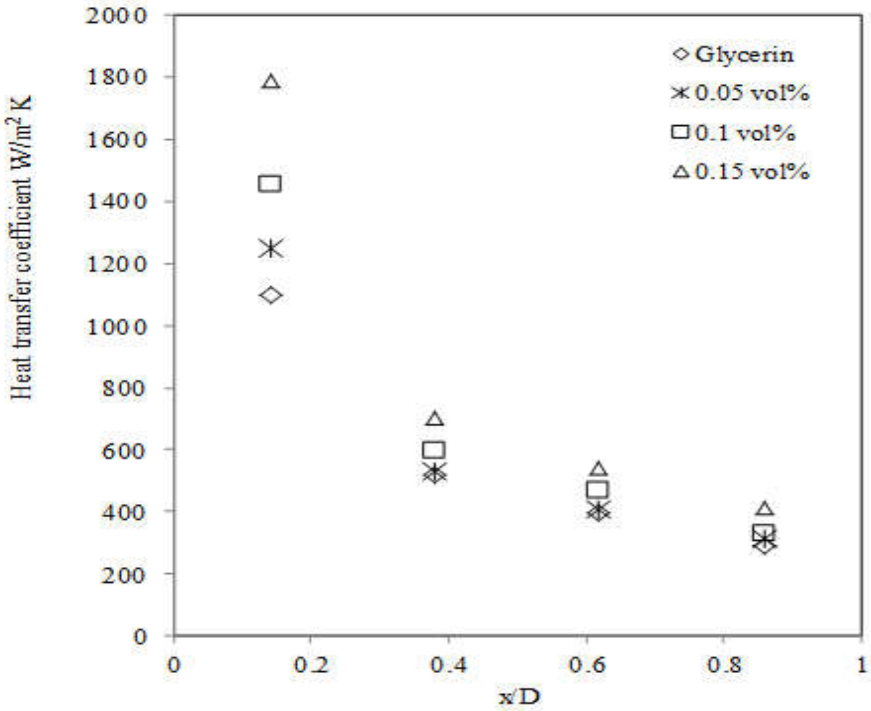

Figure 4. Axial profile of local heat transfer coefficient at Reynolds number 1200

Convective Heat Transfer Coefficient

Figure 4 shows the plot of local heat transfer coefficient against the axial distance from the entrance of the test section at Reynolds number 1200. The results clearly show that the convective heat transfer, particularly in the entrance region, is higher. The local heat transfer coefficient is also seen to increase with particle concentration. At a dimensionless length of 0.14, it is observed that the local heat transfer coefficient increases from 1100 W/m^2 K to 1789W/m^2 K at a Reynolds number of 1000 with the increase in the volume concentration of nanoparticles from 0.05% to 0.15%.At a dimensionless length of 0.38 which is the second local point, it is observed that the local heat transfer coefficient increases from 522 W/m^{2}K to 701W/m^2 K with the increase in the volume concentration of nanoparticles from 0.05% to 0.15%.At the third local point which is at a dimensionless length of 0.62,it is observed that the local heat transfer coefficient increases from 399 W/m^{2}K - 544 W/m^2 K with the increase in the volume concentration of nanoparticles from 0.05% to 0.15%. At a dimensionless length of 0.86 which is the fourth local point, it is observed that the local heat transfer coefficient increases from 522 W/m^{2}K to 701W/m^2 K with the increase in the volume concentration of nanoparticles from 0.05% to 0.15%. The enhancement in the heat transfer coefficient is 62% when 0.15% volume concentration is added to the glycerin based coolant at a Reynolds number 1000.At the local point 1 by the addition of 0.05 vol.%,0.1 vol.% and 0.15 vol.% nanoparticles were added to the glycerin based coolant, a consistent enhancement of 13%,32% and 62% is observed. As the nanoparticles are added to the base fluid the density and thermal conductivity increases while viscosity markably increases, even when compared with the enhancement of the heat transfer coefficient seems to be negligible.

Figure 5 shows variation in the temperature difference between the wall and fluid along the axial length. The graph explains the temperature difference between the bulk fluid and wall of the test section. It is observed that at a particular Reynolds number (1200) at different axial points, the temperature difference increases. As the volumetric concentration increases, the temperature difference reduces which indicates clearly that the heat transfer increases with the use of nanofluid. It is observed that the effect of wall and bulk temperature on the axial length at 0.8 is 37% higher than that of the glycerin-based coolant. By this, one can understand that the glycerin/Al_2O_3 nanofluid has a significant heat transfer absorption capacity than that of the base fluid.

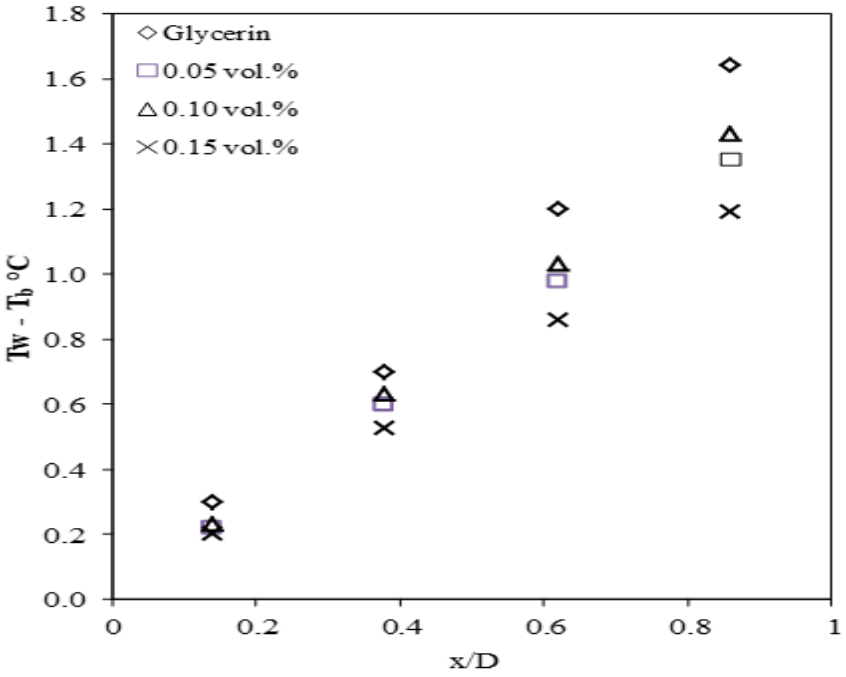

Figure 5. Effect of wall and bulk temperature on the axial length

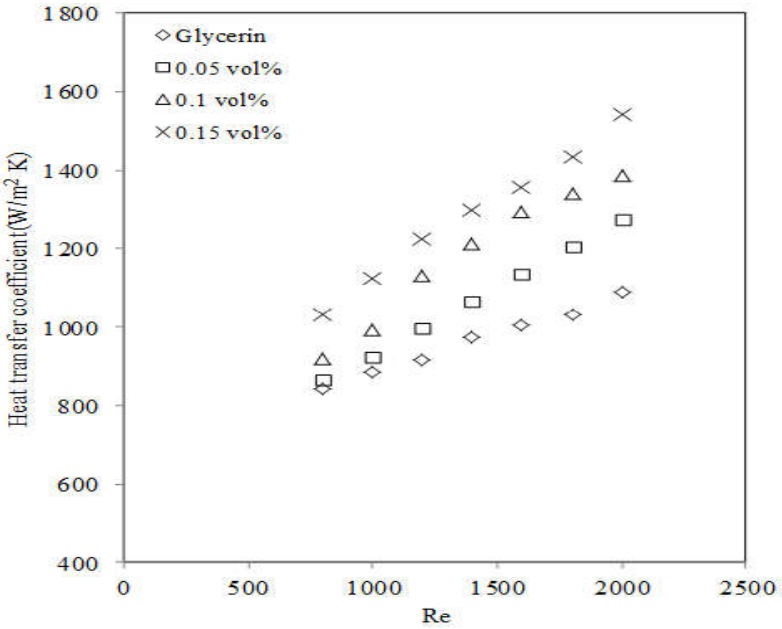

Figure 6. Variation of average heat transfer coefficient as a function of Re

Figure 6 shows the average heat transfer coefficient as a function of Reynolds number. The results clearly indicate that increase in heat transfer coefficient, as the Reynolds number and volume concentrations of glycerin/Al_2O_3 nanofluid increases. An average of 35% enhancement is observed in the laminar flow region. At Reynolds number 800, the convective heat transfer coefficient value is 843W/m^2 K for the base fluid and 1033 W/m^2 K for 0.15% of nanofluid. The enhancement in heat transfer coefficient of 22% is observed. At Reynolds number 2000 the convective heat transfer coefficient value is 1090 W/m^2 K for the base fluid and 1543W/m^2 K for 0.15% of nanofluid. The enhancement in heat transfer coefficient of 42% is observed at Reynolds number 2000. As the Reynolds number increases from 500 to 2000 the heat transfer enhancement is also increased from 28% to 42%.

Correlation for Nusselt number (Nu)

The Nusselt number basically depends on the diameter and the thermal conductivity of the fluid. It also depends on the properties such as heat capacity, viscosity and the amount of particles suspended in the liquid. A new correlation is developed to determine the Nusselt number which is a function of Reynolds number and Prandtl number and shown in Equation 16. The correlation is developed based on the experimental results of the liquid flow of the nanofluids of different volume concentrations in laminar flow regime for a constant heat flux. A multi variable linear regression is applied to determine the new correlation. The Nusselt number which is a function of Reynolds and Prandtl number is given in the following Equation 13.

$$Nu = C\ (Re)^a\ (Pr)^b \tag{13}$$

The constants C, a and b are to be determined and the Equation 14 shows the logarithmic form

$$ln \times Nu = ln\, A + b\, ln\, Re + c\, ln\, Pr \tag{14}$$

$$Q = X + bY + cZ \tag{15}$$

where, $Q = \ln Nu$, $X = \ln C$, $Y = \ln Re$, $Z = \ln Pr$

The constants C, a and b are determined by partially differentiating with respect to the constants and the new correlation is given in Equation 14

$$Nu = 0.074022\ Re^{0.929745} Pr^{0.089703} \tag{16}$$

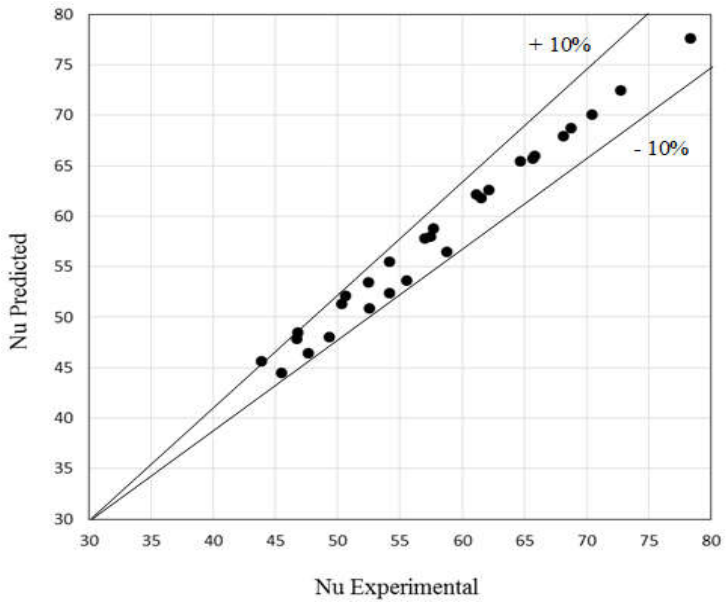

Figure 7. Experimental and predicted Nusselt number of glycerin/Al_2O_3 nanofluid

It is observed that the experimental and predicted Nusselt number for 0.05%, 0.1% and 0.15% volume concentrations are within ± 10% as shown in Figure 7.

Effectiveness of Radiator

Figure 8 shows the effectiveness of the radiator as a function of Reynolds number and volume concentrations of nanoparticles. The glycerin/Al_2O_3 nanofluid with higher concentrations are showing higher enhancement of effectiveness. The nanofluid absorption time reduces as the flow increases, which has a direct effect on the effectiveness of the radiator. It is observed that the effectiveness is varying from 0.98 to 0.69 as the Reynolds number increases from 500 to 2000. The enhancement is observed to be about 12 % at a Reynolds number of 1250 with respect to the glycerin-based coolant.

Radiator Cooling Performance

The glycerin/Al_2O_3 nanofluid having different volume concentrations at different Reynolds number are implemented throughout the experimental setup. In view of the influence of temperature on the nanofluid it is essential to know the difference between the inlet and outlet temperature of the radiator by which one can predict the thermal behavior and cooling performance. The Figure 9 shows the comparison of the radiator cooling performance when using a nanofluid at different Reynolds number. The radiator outlet temperature (ΔT) decreases as the Reynolds number increases. It is observed that the addition of nanoparticles in the base fluid has improved the absorption capacity of the radiator.

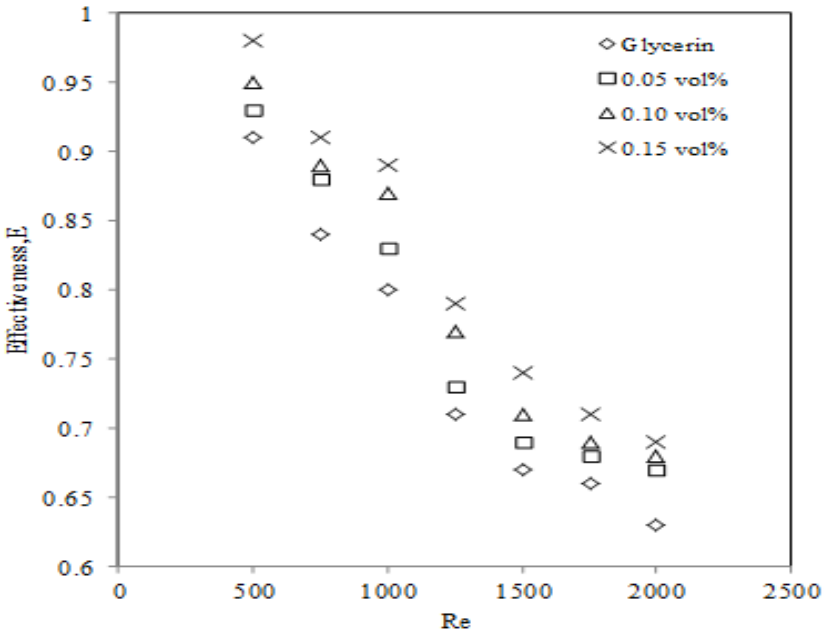

Figure 8. Effect of effectiveness with respect to Reynolds number

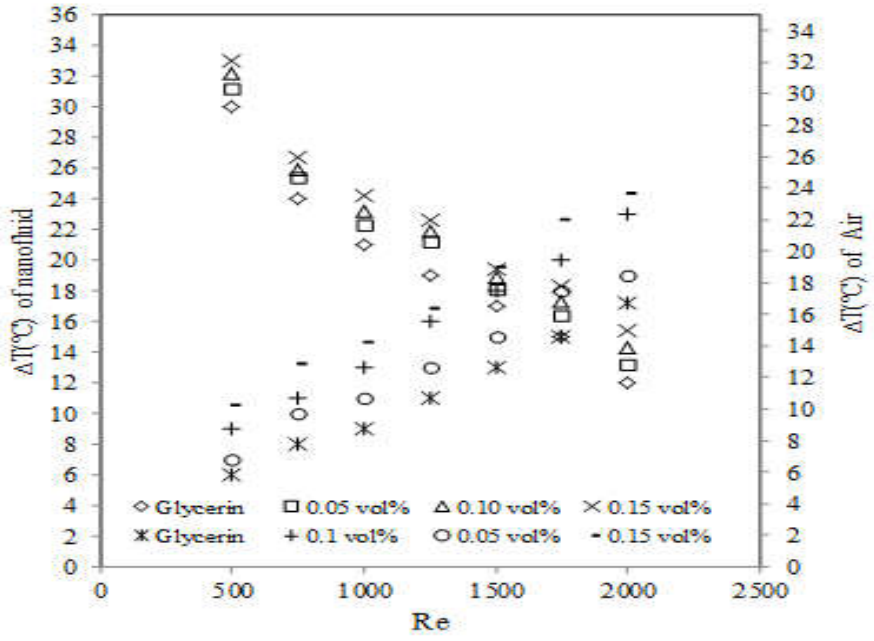

Figure 9. Variation of radiator outlet temperature with respect to Reynolds number

The temperature of the air that is absorbing the heat is clearly evident in the graph and is increasing which indicates that the amount of heat carried by the nanofluids in the radiator is carried away by the air flow.

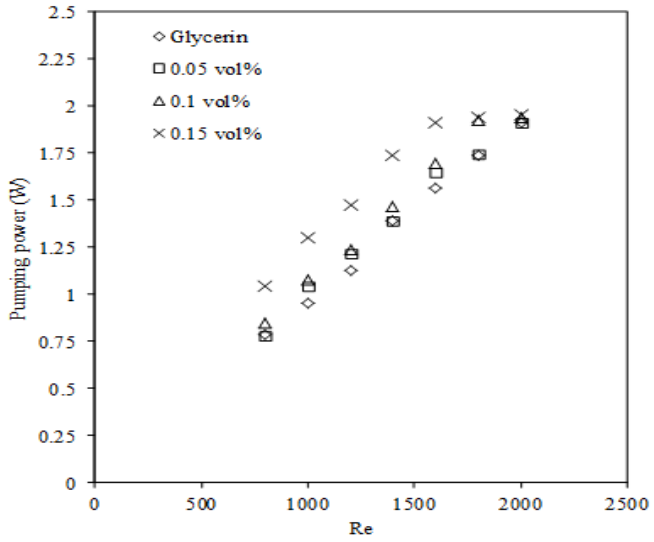

Figure 9. Pumping power as a function of Reynolds number

Pumping Power

The Figure 10 shows that the variation of pumping power is a function of Reynolds number. It is observed that the pumping power increases as the nano particles are added in the glycerin-based coolant. The enhancement in the pumping power is 11.29% at a Reynolds number of 1400 for 0.15% of nanoparticles addition. The increase in pumping power is due to the increase of viscosity of nanoparticles in the glycerin-based coolant. It is observed that the increase in pumping power is considerably lower due to the low volumetric concentration of nanoparticle. The usage of lower concentrations of nanoparticles will be an optimum solution to reduce the pumping power.

CONCLUSIONS

The Al_2O_3 nanoparticles are dispersed in glycerin-based coolant (G13) and significant enhancement in the convective heat transfer coefficient is observed in the laminar flow regime. The thermal enhancement increases with the Reynolds number as well as particle concentrations. The effectiveness of the radiator increases as the particle concentration increases. The pumping power increases as the volume concentration of the nanoparticles are added to the base fluid but is negligible due to lower volume concentrations. The experimental results indicate that the nanofluids are mainly dependent on particle concentration, flow rates and temperature. So glycerin/Al_2O_3 nanofluids possess a good potential to improve the cooling performance of the car radiator.

NOMENCLATURE

D_{vol}	Crystallized Diameter (m)
$T_{w(i)}$	Inlet Wall Temperature (°C)
$T_{f(i)}$	Inlet Fluid Temperature (°C) at the Particular Local Point
q	Heat Flux (W/m^2)
h_i	Heat Transfer Coefficient (W/m^{2}K)
T_{in}	Inlet Fluid Temperature (°C)
ρ	Fluid Density (kg/m^3)
S_x	Perimeter of the Test Section (m)
A	Cross-Sectional Area of the Tube (m^2)
C_p	Specific Heat Capacity (J/kgK)
v	Fluid Velocity (m/s)
T_{bulk}	Fluid Bulk Temperature (°C)
ε	Effectiveness

REFERENCES

[1] Xiaoke L, Changjun Z, Aihua Q. Experimental study on the thermo-physical properties of car engine coolant (water/ethylene glycol mixture type) based SiC nanofluid. Micro 2010;37:1290–4. https://doi.org/10.1016/j.icheatmasstransfer.2010.06.032.

[2] Hemmat Esfe M, Karimipour A, Yan WM, Akbari M, Safaei MR, Dahari M. Experimental study on thermal conductivity of ethylene glycol based nanofluids containing Al2O3 nanoparticles. International Journal of Heat and Mass Transfer 2015;88:728–34. https://doi.org/10.1016/j.ijheatmasstransfer.2015.05.010.

[3] Hussein AM, Bakar RA, Kadirgama K, Sharma K V. Heat transfer enhancement using nanofluids in an automotive cooling system. International Communications in Heat and Mass Transfer 2014;53:195–202. https://doi.org/10.1016/j.icheatmasstransfer.2014.01.003.

[4] Stephen USC, Eastman J. ; Enhancing thermal conductivity of fluids with nanoparticles 1995.

[5] Godson L, Raja B, Mohan Lal D, Wongwises S. Enhancement of heat transfer using nanofluids-An overview. Renewable and Sustainable Energy Reviews 2010;14:629–41. https://doi.org/10.1016/j.rser.2009.10.004.

[6] Siddiqui FA, Dasgupta ES, Fartaj A. Experimental investigation of air side heat transfer and fluid flow performances of multi-port serpentine cross-flow mesochannel heat exchanger. International Journal of Heat and Fluid Flow 2012;33:207–19. https://doi.org/10.1016/j.ijheatfluidflow.2011.12.001.

[7] Eastman JA, Choi SUS, Li S, Yu W, Thompson LJ. Anomalously increased effective thermal conductivities of ethylene glycol-based nanofluids containing copper nanoparticles. Applied Physics Letters 2001;78:718–20. https://doi.org/10.1063/1.1341218.

[8] Wen D, Ding Y. Experimental investigation into convective heat transfer of nanofluids at the entrance region under laminar flow conditions. International Journal of Heat and Mass Transfer 2004;47:5181–8. https://doi.org/10.1016/j.ijheatmasstransfer.2004.07.012.

[9] Peyghambarzadeh SM, Hashemabadi SH, Hoseini SM, Seifi Jamnani M. Experimental study of heat transfer enhancement using water/ethylene glycol based nanofluids as a new coolant for car radiators. International Communications in Heat and Mass Transfer 2011;38:1283–90. https://doi.org/10.1016/j.icheatmasstransfer.2011.07.001.

[10] Vermahmoudi Y, Peyghambarzadeh SM, Hashemabadi SH, Naraki M. Experimental investigation on heat transfer performance of Fe_2O_3/water nanofluid in an air-finned heat exchanger. European Journal of Mechanics, B/Fluids 2014;44:32–41. https://doi.org/10.1016/j.euromechflu.2013.10.002.

[11] Hussein AM, Bakar RA, Kadirgama K, Sharma K V. Heat transfer augmentation of a car radiator using nanofluids. Heat and Mass Transfer/Waerme- Und Stoffuebertragung 2014;50:1553–61. https://doi.org/10.1007/s00231-014-1369-2.

[12] Nieh HM, Teng TP, Yu CC. Enhanced heat dissipation of a radiator using oxide nano-coolant. International Journal of Thermal Sciences 2014;77:252–61. https://doi.org/10.1016/j.ijthermalsci.2013.11.008.

[13] Tharayil T, Asirvatham LG, Ravindran V, Wongwises S. Thermal performance of miniature loop heat pipe with graphene-water nanofluid. International Journal of Heat and Mass Transfer 2016;93:957–68. https://doi.org/10.1016/j.ijheatmasstransfer.2015.11.011.

[14] Ahammed N, Asirvatham LG, Wongwises S. Entropy generation analysis of graphene–alumina hybrid nanofluid in multiport minichannel heat exchanger coupled with thermoelectric cooler. International Journal of Heat and Mass Transfer 2016;103:1084–97. https://doi.org/10.1016/j.ijheatmasstransfer.2016.07.070.

[15] Ali M, El-Leathy AM, Al-Sofyany Z. The effect of nanofluid concentration on the cooling system of vehicles radiator. Advances in Mechanical Engineering 2014;2014:1–13. https://doi.org/10.1155/2014/962510.

[16] Chougule SS, Sahu SK. Comparative study of cooling performance of automobile radiator using Al_2O_3-water and carbon nanotube-water nanofluid. Journal of Nanotechnology in Engineering and Medicine 2014;5:1–6. https://doi.org/10.1115/1.4026971.

[17] Chavan D, Pise AT. Experimental investigation of convective heat transfer agumentation using Al_2O_3/water nanofluid in circular pipe. Heat and Mass Transfer/Waerme- Und Stoffuebertragung 2015;51:1237–46. https://doi.org/10.1007/s00231-014-1491-1.

[18] Angeline AA, Jayakumar J, Asirvatham LG, Wongwises S. Power generation from combusted “Syngas” using hybrid thermoelectric generator and forecasting the performance with ANN technique. Journal of Thermal Engineering 2018;4:2149–68. https://doi.org/10.18186/journal-of-thermal-engineering.433806.

[19] Asirvatham LG. Nanofluid heat transfer and applications. Journal of Thermal Engineering 2015;1:113–5. https://doi.org/10.18186/jte.93344.

[20] Kole M, Dey TK. Thermal conductivity and viscosity of Al_2O_3 nanofluid based on car engine coolant. Journal of Physics D: Applied Physics 2010;43. https://doi.org/10.1088/0022-3727/43/31/315501.

[21] Elias MM, Mahbubul IM, Saidur R, Sohel MR, Shahrul IM, Khaleduzzaman SS, et al. Experimental

investigation on the thermo-physical properties of Al_2O_3 nanoparticles suspended in car radiator coolant. International Communications in Heat and Mass Transfer 2014;54:48–53. https://doi.org/10.1016/j.icheatmasstransfer.2014.03.005.

[22] Peyghambarzadeh SM, Hashemabadi SH, Naraki M, Vermahmoudi Y. Experimental study of overall heat transfer coefficient in the application of dilute nanofluids in the car radiator. Applied Thermal Engineering 2013;52:8–16. https://doi.org/10.1016/j.applthermaleng.2012.11.013.

[23] Yu W, Xie H, Li Y, Chen L, Wang Q. Experimental investigation on the heat transfer properties of Al_2O_3 nanofluids using the mixture of ethylene glycol and water as base fluid. Powder Technology 2012;230:14–9. https://doi.org/10.1016/j.powtec.2012.06.016.

[24] Sridhara V, Satapathy LN. Al_2O_3 -based nanofluids : a review. Nanoscale Research Letters 2011:1–16.

[25] Ahammed N, Asirvatham LG, Wongwises S. Thermoelectric cooling of electronic devices with nanofluid in a multiport minichannel heat exchanger. Experimental Thermal and Fluid Science 2016;74:81–90. https://doi.org/10.1016/j.expthermflusci.2015.11.023.